Linear viscoelastic behavior of aggregated colloidal dispersions

W. Wolthers, D. van den Ende,* V. Breedveld, M. H. G. Duits, A. A. Potanin, R. H. W. Wientjes, and J. Mellema
J. M. Burgers Centre, Rheology Group, Department of Applied Physics, University of Twente, P.O. Box 217, 7500 AE Enschede, The Netherlands
(Received 16 January 1997)

The viscoelastic behavior of a depletion-flocculated dispersion of colloidal spheres is investigated at different volume fractions of the spheres, using a controlled stress and a dynamic rheometer. Combining the results, we obtain the storage G' and loss G'' moduli over a frequency range of $0.02<\omega<200$ rad/s. The measured G' gradually increases with increasing frequency, while G'' almost remains constant, indicating a broad spectrum of relaxation times. To describe and explain the observed behavior of the moduli as a function of frequency and volume fraction in terms of microscopic parameters, a microrheological model based on the fractal concept is proposed. Comparing experimental results with model calculations, we find a good agreement between the two, with physically plausible parameter values. [S1063-651X(97)02511-7]

PACS number(s): 82.70.Dd

I. INTRODUCTION

The microstructure of complex materials can be probed mechanically by viscoelastic measurements. Three types of experimental techniques can be distinguished. First, retardation experiments, where a small stress is applied and the resulting deformation J of the material is measured as a function of time. Second, relaxation experiments, where a small deformation is applied and as a function of time the stress G in the material is measured. Third, experiments can be performed in the frequency domain. In this paper the linear viscoelastic properties of our model fluid are characterized with two different experimental techniques, a retardation experiment, and a harmonic experiment, and the results are compared with each other.

The model fluid used is a mixture of monodisperse colloidal stearyl-coated spheres and a nonadsorbing polystyrene polymer dispersed in cyclohexane at 35 °C. Above a limiting value of polymer concentration, colloidal particles will aggregate as a result of attractive forces induced by a depletion of polymer molecules. The choice of this particular model fluid is based on the fact that interactions between the spheres are well defined. Light-scattering and rheological experiments [1,2] have shown for stearyl-coated silica spheres suspended in cyclohexane, that van der Waals attractions between silica cores can be neglected compared to the short-range repulsive steric forces of the surface coating. Therefore, the particles themselves behave like hard spheres. Phase experiments have shown that addition of a nonadsorbing polymer leads to a reversible attraction between the spheres. De Hek and Vrij [3,4] used the same type of model fluid as we did, and studied the polymer-induced interactions using phase and light-scattering experiments.

Although a number of authors studied viscoelastic properties of aggregated dispersions (see, for instance, Refs. [5,6]), so far only a few data are available on the frequency dependence. Patel and Russel [7] performed a combined phase separation and rheological study on polystyrene lattices phase separated by dissolved dextran polymer. They detected a low-frequency plateau in the elastic modulus for some of the samples. De Rooij *et al.* [8] investigated the elastic behavior of weakly aggregating latex dispersions. They measured (among others) the frequency dependence of the storage modulus $G'(\omega)$, and found that G' gradually increased with increasing angular frequency. The same behavior was reported by Bremer *et al.* [9] for a less well-defined aggregated system. They stated that both G' and loss modulus G'' of acid casein gels increased with angular frequency ω as $G \propto \omega^{0.15}$ over the whole frequency range investigated: $10^{-3}<\omega<10$ rad/s.

Several authors interpreted the elasticity of aggregated dispersions in terms of the fractal concept [9,10]. Although differing in details, the models depended on the assumption that the aggregated structure transmits stress through its elastic backbone (a chain of particles). From a theoretical point of view, a number of authors pointed out that, for spheres, central interactions alone can not be responsible for the static elastic behavior at rest. A simple chain with each sphere connected to two neighbors can be loaded only when it is straight, since a chain that is not straight can relax the stress by a reordering of the spheres while preserving the interparticle distances. Recently, Potanin *et al.* [11] modeled the elastic backbone as an interconnected bundle of chains of particles. Such a chain will respond to small deformations as a contorted rigid rod, and can be responsible for the observed elastic behavior at rest. In this paper we will extend this model, in order to describe our measurements of dynamic moduli as a function of frequency and volume fraction of primary particles.

The outline of the paper is as follows. In the first part of Sec. II, we will give some basic equations from linear viscoelastic theory and a method to compare the results of a retardation experiment in the time domain with those of a harmonic experiment. The second part of Sec. II contains a general description of the microrheological model. In Sec. III we will consider sample preparation and rheological experiments. The experimental results will be discussed and compared with the microrheological model in Sec. IV, and, finally, conclusions will be drawn in Sec. V.

*Author to whom correspondence should be addressed.

II. THEORY

A. Retardation and relaxation experiments

In retardation experiments (creep experiments), the strain $\gamma(t)$ in the material is measured as a function of time, after imposing a stress $\sigma(t)=\sigma_0 H(t)$, with $H(t)$ the Heaviside or unit step function. From linear viscoelastic theory [12], one can derive a general form of the retardation function $J(t)\equiv\gamma(t)/\sigma_0$:

$$J(t)=H(t)\left[J_g+\frac{t}{\eta_0}+\sum_k J_k(1-e^{-t/t_k})\right], \tag{1}$$

where J_g represents the glass compliance and η_0 the low shear limit of the steady shear viscosity. J_k and t_k are the strength and time constant of a single retardation process.

Applying a stepwise strain $\gamma(t)=\gamma_0 H(t)$ instead of a stress, one can also derive a general form of the stress $\sigma(t)$ as a function of time. The relaxation function $G(t)\equiv\sigma(t)/\gamma_0$ has the form [12]

$$G(t)=\eta'(\infty)\delta(t)+H(t)\left[G_0+\sum_k G_k e^{-t/\tau_k}\right], \tag{2}$$

where $\eta'(\infty)$ is the real part of the complex viscosity at infinite frequency, and G_0 the equilibrium modulus. G_k and τ_k are the strength and time constant of a single relaxation process.

Experiments can also be performed in the frequency domain. Applying small harmonic excitations of strain or stress to a sample, one can find the complex modulus $G^*(\omega)\equiv G'(\omega)+iG''(\omega)$ or complex compliance $J^*(\omega)\equiv J'(\omega)-iJ''(\omega)$ of the material. The functions J^* and G^* are related by $J^*(\omega)G^*(\omega)=1$ or

$$G'(\omega)=\frac{J'(\omega)}{J'^2(\omega)+J''^2(\omega)}, \tag{3}$$

$$G''(\omega)=\frac{J''(\omega)}{J'^2(\omega)+J''^2(\omega)}. \tag{4}$$

The results of creep experiments can be compared with those of harmonic experiments by using the following empirically optimized relations between $J(t)$ and $J^*(\omega)$ proposed in Ref. [13]:

$$J'(\omega)\cong[1-m(2t)]^{0.8}J_r(t), \tag{5}$$

$$J''(\omega)-\frac{1}{\omega\eta_0}\cong\left[m\left(\frac{2}{3}t\right)\right]^{0.8}J_r(t), \tag{6}$$

where $\omega=1/t$ and $m(t)\equiv d\ \ln J_r(t)/d\ \ln t$. Although Eqs. (5) and (6) were tested [13] for three different polymeric samples representing various kinds of retardation spectra $L(\tau)$, we will check the transformation of $J(t)$ to $J^*(\omega)$ with the following equations from linear viscoelastic theory [12]:

$$J_r(t)=J(t)-\frac{t}{\eta_0}=J_g+\int_{-\infty}^{+\infty}L(\tau)\left[1-\exp\left(\frac{-t}{\tau}\right)\right]\frac{d\tau}{\tau}, \tag{7}$$

$$J'(\omega)=J_g+\int_{-\infty}^{+\infty}\frac{L(\tau)}{1+(\omega\tau)^2}\frac{d\tau}{\tau}, \tag{8}$$

$$J''(\omega)=\frac{1}{\omega\eta_0}+\int_{-\infty}^{+\infty}\frac{L(\tau)\omega\tau}{1+(\omega\tau)^2}\frac{d\tau}{\tau}, \tag{9}$$

by determining $L(\tau)$ from Eqs. (8) and (9) and substituting this $L(\tau)$ in Eq. (7).

B. Microrheological model

Recently a microrheological model was proposed [11], describing linear viscoelastic properties of aggregated colloids. The shear stress in the dispersion is modeled as a sum of certain hydrodynamic and structural contributions of aggregates, where the structural part is due to interaggregate bonds. In the linear regime, as investigated in the present study, the hydrodynamic part is neglected, and the structural part is modeled by incorporating the concept of fractal aggregation into a transient network theory.

The dispersion is described as a system of overlapping aggregates, which can be interconnected by chains continuously created and broken down due to thermal processes. Most of interaggregate chains contain a junction of only two spheres. They are elastically inactive, since particles around this soft junction will relax the stress by rotating freely. Therefore, only some fraction of interaggregate chains are elastically active (rigid), and the transition of one type to the other is taken into account via kinetic equations.

One assumption of the model is that the number density of rigid interaggregate bonds N_r is small compared to the number density of aggregates. We have investigated the validity of this assumption by estimating N_r from the physical parameters of our model fluid, and found that in our case the value for N_r would exceed the number density of primary particles. This high value for N_r is due to the difference in physical parameters between our model fluid and the one studied in the paper by Potanin *et al.* [11]. Furthermore, the model only describes the limiting behavior of the viscoelastic properties, and not the frequency dependence. Therefore we will extend the model on these two points. In the next part of this section we will estimate the moduli G' and G'' as functions of the frequency and volume fraction of primary particles, avoiding detailed calculations of numerical coefficients.

1. Aggregate parameters

As before, all primary particles are assumed to be combined into aggregates. These aggregated structures transmit stress through their rigid elastic backbones, and at rest the backbone chains will form a space-filling network. The viscoelastic properties of the aggregated dispersion are (among others) a function of the volume fraction primary particles ϕ. The dependency originates from the size dependence of the aggregates on ϕ. To model this size dependence, the aggregates are described as fractal-like structures with a radius ξ, which is the radius of the smallest sphere containing all primary particles:

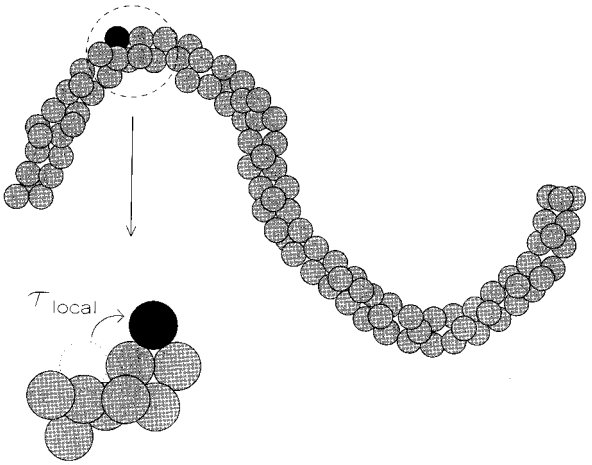

FIG. 1. The multiply connected chain.

$$N(\xi)\simeq\left(\frac{\xi}{a}\right)^{d_f}, \tag{10}$$

with N the number of particles per aggregate, a the primary particle radius and d_f the fractal dimension of the aggregate. Using Eq. (10) the average internal volume fraction of primary particles inside an aggregate is given by

$$\overline{\phi_{\rm int}}\simeq\left(\frac{\xi}{a}\right)^{d_f-3}. \tag{11}$$

Setting $\overline{\phi_{\rm int}}$ equal to the volume fraction of primary particles ϕ, yields a value for the correlation length ξ of the network. In the remainder of this section, use will be made of a mean end-to-end distance $\overline{p}$ of the rigid chains and this distance will be identified as $\simeq\xi$; hence

$$\frac{\overline{p}}{a}\simeq\phi^{1/(d_f-3)}. \tag{12}$$

2. Rigid chain parameters

The rigid elastic backbones are modeled as multiply connected chains, which consist of a bundle of primary particles containing no pivot points; see Fig. 1. The number of primary particles $N_{\rm ch}$ inside it can be related to its end-to-end distance q by

$$N_{\rm ch}\simeq\left(\frac{q}{a}\right)^{d_l}, \tag{13}$$

where d_l is an exponent, which is similar to the chemical length exponent, introduced for singly connected chains [14].

The deformation of these rigid chains is modeled in the linear regime as one of a Hookean spring with force constant k_e. So the force **f** transmitted by the chain is linear related to its elongation Δq,

$$\mathbf{f}=k_e\Delta q\frac{\mathbf{q}}{q}, \tag{14}$$

where the constant k_e is related to the value of the second derivative k_{e1} of the particle pair potential $U(r)$ in the vicinity of its minimum $k_{e1}=(\partial^2U/\partial r^2)_{r=r_{\rm min}}$ and to geometrical parameters of a chain. Modeling a chain as a contorted elastic rod with a modulus, identical to that of a compactly packed system of particles, one can find [15]

$$k_e\simeq k_{e1}\left(\frac{q}{a}\right)^{-2-d_l}. \tag{15}$$

Equation (15) describes the elasticity of a permanent chain, but we want to consider viscoelastic properties of a transient network consisting of chains with a finite life time. The chain shown in Fig. 1 loses its rigidity at a removal of any of its particles. Then a pivot point is created and particles around this point will relax the stress by a free rotation. The rigid-to-soft transition time $\tau_{\rm rs}$ can be approximated by

$$\tau_{\rm rs}\simeq\frac{\tau_{\rm local}}{N_{\rm ch}}, \tag{16}$$

where $\tau_{\rm local}$ is the mean time for one particle to exchange stable positions, as shown in Fig. 1. To find an expression for $\tau_{\rm local}$, we have made use of reaction rate theory [16]. The lowest potential barrier is achieved if a particle ''rolls'' over some of its neighbors toward a new stable position. The minimum number of bonds to be broken is z. Therefore, the total potential barrier can be approximated by $U\sim zU_c$, in which $U_c=-U(r_{\rm min})$ is the two-particle bond energy. The mean escape time $\tau_{\rm local}$ of a particle from the total potential well is then given by

$$\tau_{\rm local}\simeq\frac{12\pi^2\eta_s a}{\sqrt{-U''(l_0)U''(l_B)}}\exp[zU_c/kT], \tag{17}$$

in which a represents the particle radius and η_s is the viscosity of the polymer solution surrounding the particles ($\eta_s=2.14\times10^{-3}$ Pa s). The distances l_0 and l_B refer in our case to the stationary position of the particle and position of the barrier. At the stationary position $l_0=r_{\rm min}$, we write $U''(r_{\rm min})=zk_{e1}$. The characteristic width of the barrier $\sim a$, and therefore we set $U''(l_B)$ to zU_c/a^2.

Rheological experiments [8,9] on aggregating dispersion indicate the existence of a broad range of relaxation times, since G' increased over the whole frequency range tested $10^{-3}<\omega<10$ rad/s. Obviously, the assumption of single-type chains having one relaxation time $\tau_{\rm rs}$ is too simple. A trivial extension is assuming the chains to have a distribution $l(\overline{z})$ of mean number of bonds which have to be broken $\overline{z}$, which results in a broad spectrum of relaxation times.

3. Rheological properties of the dispersion

To estimate the rheological properties of the dispersion, we follow the standard transient network approach [17]. In this approach, the macroscopic stress tensor **T** is described as a sum of contributions from elastic chains having an end-to-end vector **q** and transmitting a force **f**. In order to obtain an expression for **T**, distribution functions describing the probability of finding a chain at a certain time with a certain end-to-end vector, are invoked. By choosing appropriate probability functions for the creation, evolution, and annihilation of chains, **T** can be calculated for any flow experiment

that obeys creeping-flow conditions. Assuming an affine relative motion of the aggregates during a small-amplitude oscillating shear flow, for the xy component of the stress tensor T^{struct} one can write

$$T_{xy}^{\text{struct}} \simeq \int\int\int (q_x f_y) g(p,\overline{z}) \exp\left[\frac{-\tau}{\tau_{\text{rs}}(p,\overline{z})}\right] d\tau\, d^3p\, d\overline{z}, \tag{18}$$

where f_y is the force transmitted at time t by the chain with an end-to-end vector $\mathbf{q}$ that has been created a time $t-\tau$ with an end-to-end vector $\mathbf{p}$; q_x is the x component of the vector $\mathbf{q}$; $g(p,\overline{z})d\tau\, d^3p\, d\overline{z}$ is the number concentration of chains created in time interval $(t-\tau, t-\tau+d\tau)$ within the configuration range $d^3p\, d\overline{z}$; and $\exp[-\tau/\tau_{\text{rs}}(p,\overline{z})]$, with $\tau_{\text{rs}}(p,\overline{z})$ as given in Eq. (16), is the survival probability at time t for a chain created at time $t-\tau$ with end-to-end vector $\mathbf{p}$ and mean number of bonds to be broken $\overline{z}$.

Using the force-deformation relation as defined for the rigid chains in Eqs. (14) and (15), one can obtain

$$q_x f_y \simeq \left(\frac{k_{e1}}{a}\right) a^3 \left(\frac{p}{a}\right)^{-d_l} \gamma_0 \exp[i\omega t](1-\exp[-i\omega\tau]), \tag{19}$$

where ω represents the angular frequency of the oscillating shear flow, i is the imaginary unit, $i^2 \equiv -1$, and γ_0 represents the amplitude of the applied harmonic shear.

A relation for $g(p,\overline{z})$ can be derived from the number density of rigid chains N_r. As stated earlier, the approach of Potanin *et al.* [11] for estimating N_r resulted in an unphysical high value using the parameters of our model fluid. It seems reasonable to assume that the creation rate $g(p,\overline{z})$ increases with N_r at low N_r, but sharply decreases as $N_r p^3$ becomes greater than unity (the motion of chains is then hindered due to overcrowding). Therefore, in equilibrium creation versus annihilation competition keeps $N_r p^3$ close to unity. As mentioned earlier, we assume the chains have a distribution of the mean number of bonds to be broken. Defining a normalized distribution $l(\overline{z})$ for the rigid chains and setting $N_r p^3$ equal to 1, we find

$$N_r(\overline{z}) = l(\overline{z}) p^{-3}, \tag{20}$$

where $N_r(\overline{z})d\overline{z}$ represents the number density of rigid chains with a mean number of bonds to be broken between $\overline{z}$ and $\overline{z}+d\overline{z}$.

To simplify the problem, we assume that for a given volume fraction of primary particles all rigid chains have about the same length $\overline{p}$, which is given by Eq. (12). Using this assumption, we can derive a relation between $N_r(\overline{z})$ and $g(p,\overline{z})$:

$$N_r(\overline{z})d\overline{z} \simeq \int_{\overline{p}-1/2\,\Delta p}^{\overline{p}+1/2\,\Delta p} g(p,\overline{z}) \exp\left[-\frac{\tau}{\tau_{\text{rs}}(p,\overline{z})}\right] d\tau\, d^3p\, d\overline{z}$$

$$\simeq g(\overline{p,z})\tau_{\text{rs}}(\overline{p,z})\overline{p^2}\Delta p\, d\overline{z} \quad \text{with} \quad \frac{\Delta p}{\overline{p}} \ll 1. \tag{21}$$

Using Eq. (20),

$$g(\overline{p,z})\tau_{\text{rs}}(\overline{p,z}) \simeq l(\overline{z}) \frac{\overline{p}^{-5}}{\Delta p}. \tag{22}$$

Integrating Eq. (18) with Eqs. (12), (19), and (22), we come to the following estimation for the dynamic modulus $G^* = T_{xy}/\gamma_0 \exp[i\omega t]$:

$$G^*(\omega) \simeq \frac{k_{e1}}{a} \phi^{(3+d_l)/(3-d_f)} \int \frac{i\omega\tau_{\text{rs}}(\phi,\overline{z})}{1+i\omega\tau_{\text{rs}}(\phi,\overline{z})} l(\overline{z}) d\overline{z}. \tag{23}$$

The dependence of the elasticity on volume fraction ϕ in Eq. (23) is the same as the well-known scaling relation usually attributed to Ball and Brown (unpublished, but see Ref. [6]).

Transforming $\overline{z}$ into τ with Eqs. (12), (13), (16), and (17), one can obtain

$$G^*(\omega) \equiv \int \frac{d\tau}{\tau} H(\tau) \frac{(\omega\tau)^2 + i\omega\tau}{1+(\omega\tau)^2}, \tag{24}$$

in which $H(\tau)$ represents the relaxation spectrum [12], which is in our case given by

$$H(\tau) = C_1 \frac{k_{e1}}{a} \frac{kT}{U_c} l(\overline{z}) \phi^{(3+d_l)/(3-d_f)} \quad \text{and} \quad \overline{z} = \frac{kT}{U_c} \ln\left[\frac{\tau}{\tau_1}\right], \tag{25}$$

with

$$\tau_1 = C_2 \frac{12\pi^2 \eta_s a^2}{\sqrt{k_{e1} U_c}} \phi^{d_l/(3-d_f)}. \tag{26}$$

The constants C_1 and C_2 incorporate all neglected numerical coefficients and have to be of order unity. The weak dependence of τ_1 on z has been left out of consideration in the analysis.

III. EXPERIMENT

A. Sample preparation

The stearyl-coated silica particles were synthesized in two steps. First, spherical silica cores were prepared by hydrolysis of tetraethoxysilane in ethanol, according to the method described in Ref. [18]. Subsequently, the silica cores were coated by etherification of the surface silanol groups with stearyl alcohol, using the method described in Ref. [19]. The resulting particles are easily dispersible in apolar solvents such as cyclohexane. The particle size distribution was determined with transmission electron microscopy. Eighty particles were counted, giving a mean radius of 30.5 nm with a standard deviation of 2.5 nm. The particle mass density was determined gravimetrically, and was found to be $\rho_s = 1.660 \pm 0.010$ g cm^{-3}.

After addition of enough polystyrene (mass density 1.05 ± 0.01 g cm^{-3}), the silica particles will aggregate due to the phenomenon of depletion flocculation. This model system contains the same ingredients as the one studied by de Hek and Vrij [3,4], and for a discussion of the phase diagram we refer to their work (see also Ref. [20]). In the present study, the ''continuous phase'' contained 126 gram polystyrene per liter, which is about two times as large as the mini-

mum amount needed to induce phase separation (so the system is in the two-phase region far away from the phase boundary). De Hek and Vrij [4] also performed light-scattering experiments on dilute dispersions. Their measurements showed a negative adsorption of the polymer molecules at the silica particles interface, which is the origin of the depletion attraction. The polystyrene was obtained from the Tosoh corporation. The manufacturer gave the following values for the molar masses: $M_w = 5970$ (g/mole) and $M_w/M_n = 1.02$.

Samples were prepared by first drying the silica particles under a nitrogen stream and at a temperature of 60 (°C). Hereafter the dried particles were added to a polystyrene solution in cyclohexane. The required amounts were calculated using the mass densities, and assuming no excess mixing volumes. The samples were contained in glass screw bottles. After the addition of dried silica, a poly(tetra-fluoroethylene) (PTFE)-coated bar was added, and the samples were mixed by turning end over end for one day. In order to obtain a reproducible starting point, aggregates must be broken down to primary particles as much as possible. Therefore the sample was very thoroughly mixed for 3 min with a whirl mixer. With this procedure we were able to reduce the reproducibility error to about 50%.

We have calculated the primary particle interactions as in Ref. [21], and found for this slightly different sample the following values for the spring constant of the two-particle bond and particle bond energy: $k_{e1} = 0.48$ N/m and $U_c = 9.3$ kT.

B. Creep experiments

For the creep experiments we used a controlled stress rheometer with a double-gap geometry, capable of applying small shear stresses (down to ~ 1 mPa), and detecting small angular displacements (down to $\sim 10^{-6}$ rad). The instrument was developed in our laboratory [22]. During measurements, suspensions were held at 35.0 °C (the θ temperature of polystyrene in cyclohexane). The measurements were carried out for six different volume fractions of primary particles; $\phi = 5.0\%$, 6.5%, 8.0%, 10.0%, 13.0%, and 16.0%. The reproducibility of the whole experiment was checked by measuring different samples with the same composition.

The creep experiments were conducted after a waiting period of 20 min, to allow for the formation of a network. This time was, in an earlier study [23], found to be long enough for restructuring processes in the absence of strong flow fields to take place, and was verified in the present study to be short enough to avoid significant effects of aggregate sedimentation. A small stress was applied for a certain period of time (ranging between 60 and 120 s, depending on volume fraction of primary particles). During this period the angular displacement was recorded every 0.5 s, and the elastic recoil to a new position was measured in the same way during more than 250 s after cessation of the applied stress. The measured angular displacement had to be corrected for a linear drift. To this end, we determined the slopes of ten data points which were measured before and after the creep experiment. Hereafter, the measured displacement was corrected with the mean slope.

To check the linearity of stress-strain relation, we started at the lowest possible value for the applied stress which was then increased until a critical stress, whereat the sample started to behave nonlinearly. The value of the critical stress was found to be an increasing function of the volume fraction of primary particles, and ranged in our case between values of 5 and >500 mPa. The latter value is the upper limit for the stress which can be applied by the controlled stress rheometer.

C. Dynamic experiments

The dynamic experiments were performed with a controlled strain rheometer, capable of applying small-amplitude harmonic excitations. The home-made instrument [24] is suitable for measuring the dynamic moduli of a fluid in shear flow, but for the present investigation we only measured dynamic moduli at rest. The measurements were started after a waiting period of 20 min. The storage and loss moduli were measured in the frequency range between 0.1 and 30 Hz, and a check on the limits of linearity was performed by varying the strain.

Experiments were done at 35.0 °C, and, to avoid vaporization of solvent, a vapor trap was used. The dynamic measurements were performed for three different volume fractions; $\phi = 10.0\%$, 13.0%, and 16.0%. To investigate the reproducibility of the whole experiment, at every volume fraction three different samples with the same composition were prepared and measured.

IV. RESULTS AND DISCUSSION

A. Creep experiments

For each volume fraction of the experimental data, the angular displacement $\theta(t)$ as a function of time for a number of shear stresses σ_0, were handled in the following way. If the sample behaves linear, the mean shear deformation γ in the two gaps of the Couette geometry is given by the small gap approximation:

$$\gamma(t) = 10.7[\theta(t) - \theta(0)], \tag{27}$$

where $\theta(0)$ designates that all displacements are measured relative to the original zero position. Using $\gamma(t)$, the retardation function $J(t) \equiv \gamma(t)/\sigma_0$ was calculated, and Fig. 2 shows a typical result for a creep experiment at $\phi = 8\%$.

The figure shows that our model fluid behaves elastically at fast deformations and viscously at slow deformations, and from the nonzero value for η_0 one can conclude that the G_0 of our fluid is zero. Using Eq. (1), we determined values for the steady-state compliance J_e, glass compliance J_g, and viscosity η_0 from the $J(t)$ curves. From each measurement, values for J_e, J_g, and η_0 can be obtained in two ways (motor on and off). In the case of motor on, values of J_e and η_0 were determined from fitting the data with Eq. (1), setting k equal to 2. In the case of motor off, J_e and η_0 were determined from the last data point, as indicated in Fig. 2. The instantaneous jump J_g after imposing and releasing the stress was estimated by a linear extrapolation of the first two data points. The glass compliances determined in this way should be considered as upper bonds of the real values. Both ways

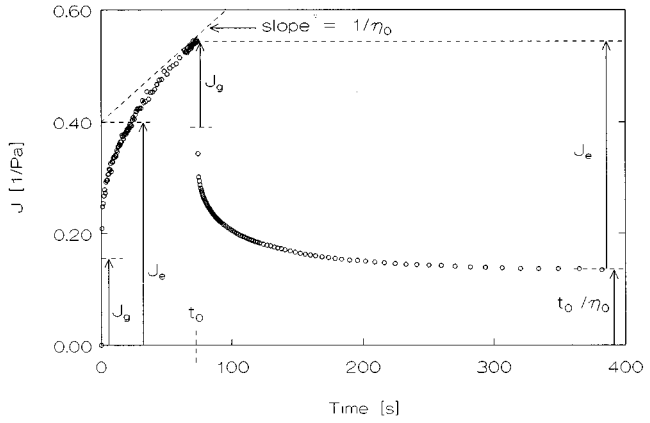

FIG. 2. Example of a creep experiment ($\phi=8\%$). The retardation function J is plotted as a function of time.

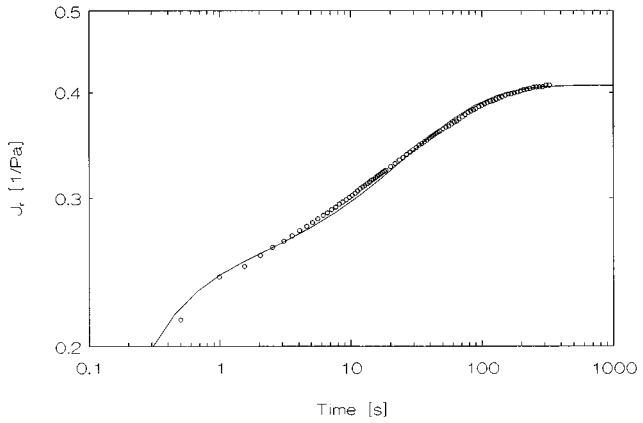

FIG. 3. Recovery creep compliance J_r ($\phi=8\%$) as a function of time. The symbol [○] represents the experimental data and the solid line is the calculated $J_{r,\mathrm{check}}(t)$; see text.

(motor on and off) of obtaining J_e, J_g, and η_0 gave the same result within the experimental error.

The linearity of different measurements was checked by comparing the obtained values of J_e, J_g, and η_0 as a function of applied shear stress σ_0. The number of linear measurements per sample ranged from three for the lowest to seven for the highest value of ϕ, and the average results of the measurements are listed in Table I. To test the reproducibility of the whole experiment, some samples ($\phi=6.5\%$, 8.0%, and 16%) were freshly prepared a second time, and subjected to the same procedures. From the differences between samples of the same composition, the systematic errors in J_e, J_g, and η_0 were all estimated to be approximately 50%. We ascribe these errors to differences in shear history, which occur during the filling of the rheometer; also see Ref. [24].

Conversion to frequency domain

In order to compare the results of the creep experiments with those of the dynamic relaxation experiments, we converted the retardation function $J(t)$ to the frequency domain. To do so, we determined $J_r(t)$ from the recovery part of a retardation experiment and as an example the data [○] for $\phi=8\%$ are shown in Fig. 3. A computer program was used to obtain $m(t)\equiv d\ \ln J_r(t)/d\ \ln t$ from a spline function fit to the data, and $J^*(\omega)$ was subsequently calculated from Eqs. (5) and (6). Because of limitations on sampling times with the creep rheometer, fast retardation processes cannot be observed with this instrument. The minimum time scale is about 1 s, which corresponds to an angular frequency ω of 1 rad/s in the frequency domain. As mentioned earlier, we periodically increased the stress during the creep experiments until a value was reached where the response became nonlinear. From Fourier transform theory we obtained a lower bond for ω of 0.02 rad/s for the creep experiments.

TABLE I. The values for J_e, J_g, η_0, and τ_m as a function of ϕ.

ϕ [%]	J_e (1/Pa)	J_g (1/Pa)	η_0 (Pa s)
5.0	3.0×10^{0}	8.9×10^{-1}	5.0×10^{1}
6.5	8.9×10^{-1}	4.3×10^{-1}	2.2×10^{2}
6.5	6.5×10^{-1}	2.4×10^{-1}	2.2×10^{2}
8.0	4.1×10^{-1}	1.7×10^{-1}	5.2×10^{2}
8.0	3.5×10^{-1}	1.2×10^{-1}	3.4×10^{2}
10.0	1.3×10^{-1}	5.2×10^{-2}	1.2×10^{3}
13.0	1.6×10^{-2}	5.6×10^{-3}	1.4×10^{4}
16.0	4.2×10^{-3}	1.5×10^{-3}	3.3×10^{4}
16.0	3.2×10^{-3}	1.3×10^{-3}	8.9×10^{4}

Although Plazek, Raghupathi, and Orbon [13] tested the empirical relations (5) and (6) for different types of retardation spectra $L(\tau)$, we also checked the transformation for all volume fractions in the following way. Using Eqs. (8) and (9), we determined the spectrum $L(\tau)$ from a fit to $J^*(\omega)$, and calculated $J_{r,\mathrm{check}}(t)$ from Eq. (7). Figure 3 shows the good agreement between $J_{r,\mathrm{check}}(t)$ (solid line) and the original $J_r(t)$ data, indicating that the method of Ref. [13] is also suitable for our data.

B. Dynamic experiments

All dynamic measurements were repeated twice with fresh samples, and again we found systematic differences between the mechanical response of same samples of about 50%. The applied strains were smaller than 10^{-3} in all experiments, this being the upper limit of linearity determined from varying the strain. The angular frequency ω ranged between the values 0.7 and 200 rad/s, and in Figs. 4 and 5 the results of the dynamic moduli are plotted as a function of ω. Since dynamic moduli are usually plotted and interpreted on a logarithmic scale, we have used the following average over repeated measurements:

$$\ln\overline{G^*}(\omega)=\frac{1}{n}\sum_{i=1}^{n}\ln G_i^*(\omega). \tag{28}$$

The results of the dynamic measurements (carried out in the frequency domain) can be compared with the creep experiments (time domain). The measurement ranges of both instruments are not the same; the creep experiments focus more on slower processes compared to the dynamic measurements (0.02–1 against 0.7–200 rad/s). In the Sec. IV A we discussed the conversion of creep data $J(t)$ to $J^*(\omega)$. From

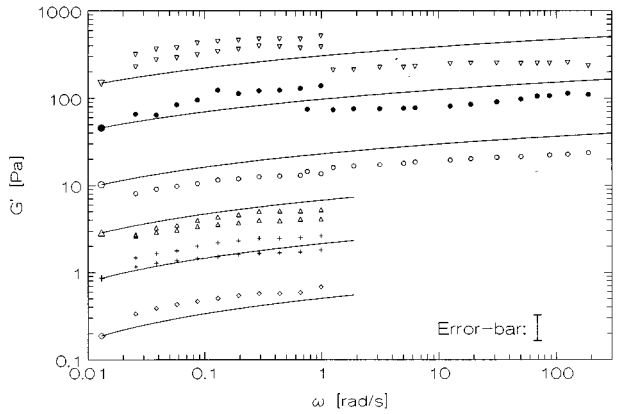

FIG. 4. The storage moduli G' obtained with the creep ($0.02<\omega<1$ rad/s) and dynamic rheometer ($0.7<\omega<200$ rad/s) as a function of angular frequency ω. The symbols represent the results for $\phi=5.0\%$ ($\diamond$), 6.5% (+), 8.0% ($\triangle$), 10% ($\bigcirc$), 13% ($\bullet$), and 16% ($\triangledown$). The solid lines represent Eq. (24) with $d_l=1$, $d_f=2.25$, $\overline{z_{\max}}=3$, $C_1=0.6$, and $C_2=0.1$.

this complex compliance function $J^*(\omega)$ we calculated a complex modulus $G^*(\omega)$ from Eqs. (3) and (4), and the results are also shown in Figs. 4 and 5.

The figures show that both instruments give the same results within the systematic error of 50%. For $\phi=10\%$ the connection is very good, and in the case of $\phi=13\%$ and 16% the curves are somewhat shifted, but the results still agree. The results for $\phi=10\%$ show that G' gradually increases with angular frequency as $G'\sim\omega^{0.14}$, which is almost the same slope as the measurements on other aggregated systems [8,9]. The data for G'' exhibit a great deal of scattering, especially at low frequencies, but we conclude that G'' remains constant within experimental errors over almost the whole frequency range tested. Only for $\omega>30$ rad/s do the loss moduli seem to increase with increasing frequency.

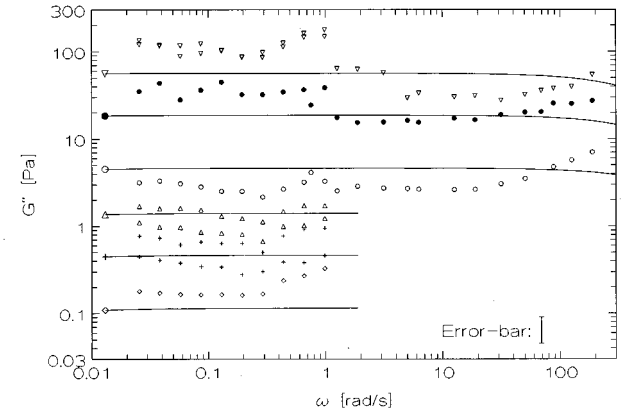

FIG. 5. The loss moduli G'' obtained with the creep ($0.02<\omega<1$ rad/s) and dynamic rheometer ($0.7<\omega<200$ rad/s) as a function of angular frequency ω. The symbols represent the results for $\phi=5.0\%$ ($\diamond$), 6.5% (+), 8.0% ($\triangle$), 10% ($\bigcirc$), 13% ($\bullet$), and 16% ($\triangledown$). The solid lines represent Eq. (24) with $d_l=1$, $d_f=2.25$, $\overline{z_{\max}}=3$, $C_1=0.6$, and $C_2=0.1$.

C. Comparison of model and experiment

In Sec. II B an expression [Eq. (24)] was derived from which we can calculate the complex dynamic modulus G^* as a function of frequency ω and volume fraction of primary particles ϕ. In this section we will check whether we can describe our experimental data with physically acceptable values for the defined but not yet quantified parameters: d_l, d_f, and $l(\overline{z})$. The value for d_l must range between 1 and 1.6. The upper bond corresponds with a self-avoiding random walk. For simplicity we will set d_l equal to unity.

The fractal dimension of aggregates d_f determines the dependence of the dynamic moduli on volume fraction of primary particles; see Eq. (23). We found the best agreement between calculations and experimental data for $d_f=2.25\pm0.02$. The error estimate was obtained by considering the sensitivity of the model for the value of d_f. From diffusion-limited cluster-cluster aggregation without internal restructuring, fractal dimensions of about 1.8 are expected, but restructuring leads to higher values for d_f. The obtained value for d_f is rather independent of the choice of the backbone dimension d_l, which must range between 1.0 and 1.6. If one takes $d_l=1.6$ instead of 1.0, one will find 2.15 instead of 2.25 for d_f. The obtained value for d_f is lower than the $d_f=2.34\pm0.02$ we obtained earlier for a similar system in nonlinear shear experiments [24], so the results are only roughly in agreement. This is mainly due to the different sample histories in the different experiments.

The broad spectrum of relaxation times is modeled with the following normalized rectangular distribution $l(\overline{z})$ of mean number of bonds which have to be broken, in order to transform the chain from rigid to soft:

$$l(\overline{z})=\begin{cases}0 & \text{for } \overline{z}<1\\ (\overline{z_{\max}}-1)^{-1} & \text{for } 1\leqslant\overline{z}\leqslant\overline{z_{\max}}\\ 0 & \text{for } \overline{z}>\overline{z_{\max}},\end{cases}\tag{29}$$

where $l(\overline{z})d\overline{z}$ is the probability of a chain to have a mean number of bonds to be broken between $\overline{z}$ and $\overline{z}+d\overline{z}$. The choice of a rectangular pulse distribution function is based on the experimental observation that G'' of our model fluid is almost constant over the whole frequency range tested; see Sec. IV B. In the proposed microrheological model this can be accomplished by using a $l(\overline{z})$ as defined in Eq. (29). We also tried a Gaussian distribution, but the experimentally observed constant G'' is not obtained with a Gaussian distribution. The rigid-to-soft transition process described in Sec. II B gives a physical lower bond ($\overline{z}=1$) for the distribution, whereas the higher bond $\overline{z_{\max}}$ determines the ratio between G' and G'' and magnitude of the longest relaxation time. The best agreement was found with $\overline{z_{\max}}=3$. This value for $\overline{z_{\max}}$ is physically reasonable; see Fig. 1.

The results of the calculations (with $C_1=0.6$ and $C_2=0.1$) are also plotted in Figs. 4 and 5. One can see that the frequency dependence of the storage modulus G' is described very well by the microrheological model. The volume fraction dependence is also caught by the model; at some volume fractions the theoretical curves exhibit an offset, but they still describe the experimental results within the systematic error bar. The calculations for loss moduli G'' are also in reasonable agreement with the experimental data, but

the model does not include the observed increase of G'' for $\omega > 30$ rad/s. Some premature modeling showed that this increase of G'' at higher frequencies can be attributed either to the internal deformation of viscoelastic aggregates or to a damping of the oscillating movement of rigid chains by the fluid which surrounds them.

V. CONCLUSIONS

In this paper the linear viscoelastic properties of an aggregated dispersion have been explored. We have determined the rheological properties using two different rheometers, a controlled stress and a harmonic rheometer, and the experimental data have been compared with each other. Both instruments gave the same results within a systematic experimental error, which is rather large. We ascribe these systematic errors to differences in shear history, which occur during the filling of the rheometer. We found that the storage modulus gradually increases with angular frequency as $G' \sim \omega^{0.14}$, while the loss modulus G'' remains constant within the experimental error over almost the whole frequency range tested ($0.02 < \omega < 200$ rad/s). These two observations indicate the existence of a large number of relaxation processes with a broad spectrum (four decades) of relaxation times.

The properties of the fluid at rest can be described satisfactorily with a microrheological model based on the fractal concept. The model we used is an extension of the work of Potanin *et al.* [11], which was modified in two ways. First of all, it is assumed that all aggregates are incorporated in the space-filling network. This was appropriate and necessary since calculations with the original model revealed that for our aggregated system, the assumption of freely moving aggregates is no longer valid. Second, a distribution of the mean number of bonds to be broken $\bar{z}$ of the rigid network chains was introduced. This was necessary to describe the broad relaxation spectrum, which was found experimentally.

The extended model describes the experimental results for the complex modulus as a function of frequency and volume fraction of primary particles within the experimental error and with physically plausible values for the parameters used. The fractal dimension was found to be lower than the value obtained from nonlinear measurements on a slightly different silica sample [24].

ACKNOWLEDGMENTS

The authors wish to acknowledge I. Stufken for her work on the synthesis of the stearyl coated silica particles. The work described in this paper is part of the research program of the Foundation for Fundamental Research on Matter (FOM), which is financially supported by the Netherlands Organization of Scientific Research (NWO).

[1] A. Vrij, J. W. Jansen, J. K. G. Dhont, C. Pathmananoharan, M. M. Kops-Werkhoven, and H. M. Fijnaut, Faraday Discuss. Chem. Soc. **76**, 19 (1983).
[2] C. G. de Kruif, E. M. F. van Iersel, A. Vrij, and W. B. Russel, J. Chem. Phys. **83**, 4717 (1985).
[3] H. de Hek and A. Vrij, J. Colloid Interface Sci. **84**, 409 (1981).
[4] H. de Hek and A. Vrij, J. Colloid Interface Sci. **88**, 258 (1982).
[5] J. W. Goodwin R. W. Hughes, S. J. Partridge, and C. F. Zukoski, J. Chem. Phys. **85**, 559 (1986).
[6] R. Buscall, P. D. A. Mills, J. W. Goodwin, and D. W. Lawson, J. Chem. Soc. Faraday Trans. **84**, 4249 (1988).
[7] P. D. Patel and W. B. Russel, J. Colloid Interface Sci. **131**, 192 (1989).
[8] R. de Rooij, D. van den Ende, M. H. G. Duits, and J. Mellema, Phys. Rev. E **49**, 3038 (1994).
[9] L. G. B. Bremer, B. H. Bijsterbosch, R. Schrijvers, T. van Vliet, and P. Walstra, Colloids Surface **51**, 159 (1990).
[10] P. D. Patel and W. B. Russel, Colloids Surface **31**, 355 (1988).
[11] A. A. Potanin, R. de Rooij, D. van den Ende, and J. Mellema, J. Chem. Phys. **102**, 5845 (1995).
[12] N. W. Tschoegl, *The Phenomenological Theory of Linear Viscoelastic Behavior* (Springer-Verlag, Berlin, 1990).
[13] D. J. Plazek, N. Raghupathi, and S. J. Orbon, J. Rheol. **23**, 477 (1979).
[14] R. Jullien and R. Botet, *Aggregation and Fractal Aggregates* (World Scientific, Singapore, 1987).
[15] R. de Rooij, A. A. Potanin, D. van den Ende, and J. Mellema, Colloid J. **56**, 476 (1994).
[16] P. Hänggi, P. Talkner, and M. Borkovec, Rev. Mod. Phys. **62**, 251 (1990).
[17] H. Kamphuis, R. J. J. Jongschaap, and P. F. Mijnlieff, Rheol. Acta **23**, 329 (1984).
[18] W. Stöber, A. Fink, and E. Bohn, J. Colloid Interface Sci. **26**, 62 (1968).
[19] A. K. van Helden, J. W. Jansen, and A. Vrij, J. Colloid Interface Sci. **81**, 354 (1981).
[20] W. C. K. Poon, J. S. Selfe, M. B. Robertson, S. M. Ilett, A. D. Pirie, and P. N. Pusey, J. Phys. (France) **3**, 1075 (1993).
[21] W. Wolthers, D. van den Ende, M. H. G. Duits, and J. Mellema, J. Rheol. **40**, 55 (1996).
[22] D. van den Ende, C. Blom, and J. Mellema, in *Theoretical and Applied Rheology*, edited by P. Moldenaers and R. Keunings (Elsevier, Amsterdam, 1992), Vol. 2, p. 1017.
[23] W. Wolthers, M. H. G. Duits, D. van den Ende, and J. Mellema, J. Rheol. **40**, 799 (1996).
[24] J. Zeegers, D. van den Ende, C. Blom, E. G. Altena, G. J. Beukema, and J. Mellema, Rheol. Acta **34**, 606 (1995).